Depletion-induced surface alignment of asymmetric diblock copolymer in selective solvents

Rong Wang,[1,a)] Yeng-Long Chen,[2] Jinglei Hu,[1] and Gi Xue[1,b)]
[1]*Department of Polymer Science and Engineering, Nanjing National Laboratory of Microstructures, School of Chemistry and Chemical Engineering, Nanjing University, Nanjing 210093, People's Republic of China*
[2]*Institute of Physics and Research Center for Applied Sciences, Academia Sinica, Taipei 11529, Taiwan*

(Received 22 January 2008; accepted 23 June 2008; published online 31 July 2008)

Phase separation of asymmetric diblock copolymer near surfaces in selective solvents is theoretically investigated by using the real-space version of self-consistent field theory (SCFT). Several morphologies are predicted and the phase diagram is constructed by varying the distance between two parallel hard surfaces (or the film thickness) W and the block copolymer concentration f_P. Morphologies of the diblock copolymer in dilute solution are found to change significantly with different film thicknesses. In confined systems, stable morphologies found in the bulk solution become unstable due to the loss of polymer conformation entropy. The vesicle phase region contracts when the repulsive interaction between the blocks is strong (strong segregation regime). The mixture of vesicles, rodlike and spherelike micelles and the mixture of vesicles and sphere-like micelles disappear in contrast to the weakly segregating regime. The walls strongly affect the phase separation of block copolymer in selective solvent, and the depletion layer near the surface contributes much to the micelle formation of the block copolymer. Interestingly, the self-assembled morphologies stay near the walls with the distance on the order of the radius of gyration of the block copolymer. The oscillation of the polymer distribution near the walls allows the surface phase separation to be observed due to the strong repulsion between the blocks A and B. © *2008 American Institute of Physics*. [DOI: 10.1063/1.2957746]

I. INTRODUCTION

Depletion interaction widely exists in polymer-colloid mixtures, at surfaces and interfaces, and has attracted increasing attention.[1,2] And we know block copolymers can microphase separate into a wide range of highly ordered nanoscale morphologies that aid in the design of desirable and functional nanomaterials. The presence of a surface or interface can strongly influence the microdomain morphologies and the kinetics of microdomain ordering of block copolymers. Does the depletion effect near the surfaces cause some new phenomena for block copolymers in solution? In general, phase separation is accompanied by a minimization of the interfacial area of contact between dissimilar phases resulting in a reduction of the enthalpy, which is balanced by a reduction of the conformational entropy of the chains. Therefore, the complex and rich-ordered microphase depend on the molecular parameters, such as the block composition, interaction energies between distinct blocks, and the architectures of the block copolymers.

Confinement of diblock/triblock copolymers between parallel solid walls, or in a thin film, has been extensively studied.[3,4] Surface and solvent effects play important roles in such systems. Solvent-influenced ordering has been exploited to control the morphology of block copolymer thin films without any thermal treatment.[5] The adsorption of diblock copolymers from a selective solvent onto a flat solid substrate also results in the formation of laterally ordered microdomains.[6] Much of the current work focus on the influence of surfaces or interfaces on the morphology of symmetric diblock copolymers, $f=0.5$.[7] The lamellae morphology of block copolymers can align either parallel or perpendicular to the surfaces depending on the film thickness and the wetting properties of the confining surfaces.[8] Relatively little work has been done on the morphology of asymmetric block copolymers thin films until recently.[4,9] The results show that strong confinement has been shown to lead to an interesting variety of morphologies.

The morphologies or self-assemblies of the amphiphilic highly asymmetric diblock or triblock copolymer with minor end blocks in dilute solution have also been widely studied experimentally[10,11] and even theoretically.[12–15] Asymmetric block copolymers can form vesicles and different micelles such as spherelike and rodlike micelles in selective solvents.[11,14,16] Among these microstructures, vesicles are of fundamental and practical interests as they have many potential applications as microreactors, microcapsules, and drug delivery systems.[17] However, there has been little consideration of the self-assemblies of block copolymers in dilute solution in confined systems, which are of interest in many biological systems. The phase behavior of block copolymer in dilute solution may be very different from that in the bulk. A hard surface or interface will induce polymer depletion, which can lead to local concentration gradients and solution phase separation under the appropriate conditions.[18,19]

[a)]Electronic mail: rong_wang73@hotmail.com.
[b)]Electronic mail: xuegi@nju.edu.cn.

Based on the recent development of self-consistent field theory (SCFT) for the study of morphologies (e.g., two dimensional circular and linear micelles corresponding to vesicle/spherelike and rodlike micelles in three dimensions) of the amphiphilic block copolymer in dilute solution,[12–14,20] we investigate the phase behavior of confined asymmetric diblock copolymers in solution in a parallel slit. Following our previous work,[21] we further extend theoretical consideration to the depletion-induced phase transition of block copolymers in strong segregation condition in selective solvents. The influences of the slit height and the concentration on block copolymer morphology are studied systematically and the phase diagram is constructed. We briefly introduce the SCFT formulation used in our study in the next section. In Sec. III, the results of the calculations and simulations are presented. And a brief summary and conclusion is also given in Sec. IV.

II. THEORETICAL METHOD

A mixture of n_P linear AB diblock copolymers with n_s solvent molecules confined between two parallel hard surfaces is considered in the paper. Each copolymer chain consists of N segments with compositions (average volume fractions) f_A and f_B ($f_B=1-f_A$), respectively. We assume the mixture is incompressible, with each polymer segment occupying a fixed volume ρ_0^{-1} and each solvent molecule taking the same volume $\nu_S=\rho_0^{-1}$. Thus, the total volume of the system is $V=n_PN/\rho_0+n_S\nu_S$, the volume fraction of the AB diblock copolymer is $f_P=n_pN/V\rho_0$ and that of the solvent is $f_S=1-f_P$. Furthermore, we assume that the A and B segments have the same segment length a.

In the SCFT one considers the statistics of a single copolymer chain in a set of effective chemical potential fields w_i, where i represents block species A, B, or solvent S. These chemical potential fields, which represent the actual interactions between different components, are conjugated to the segment density fields, ϕ_i, of different species i. The free energy of the system is given by

$$\begin{aligned}\frac{\dot{N}F}{k_BT\rho_0V} &= -f_p\ln(Q_p/f_pV) - Nf_S\ln(Q_S/f_SV) - 1/V \\ &\times\int d\mathbf{r}[w_A\phi_A + w_B\phi_B + w_S\phi_S \\ &+ \xi(1-\phi_A-\phi_B-\phi_S)] + 1/V \\ &\times\int d\mathbf{r}[\chi_{AB}N\phi_A\phi_B + \chi_{AS}N\phi_A\phi_S \\ &+ \chi_{BS}N\phi_B\phi_S], \end{aligned} \tag{1}$$

where χ_{ij} is the Flory–Huggins interaction parameter between species i and j, and ξ is the Lagrange multiplier (which acts as a pressure). $Q_P=\int d\mathbf{r}q(\mathbf{r},1)$ is the partition function of a single chain in the effective chemical potential fields w_A and w_B. $Q_S=\int d\mathbf{r}\exp(-w_S(\mathbf{r})/N)$ is the partition function of the solvent in the effective chemical potential field w_S. The fundamental quantity to be calculated in mean-field studies is the chain propagator $q(\mathbf{r},s)$, which represents the probability of finding the end of a segment with contour length s at position $\mathbf{r}$. $q(\mathbf{r},s)$ satisfies a modified diffusion equation using a flexible Gaussian chain model,[22]

$$\frac{\partial}{\partial s}q(\mathbf{r},s) = \frac{Na^2}{6}\nabla^2q(\mathbf{r},s) - wq(\mathbf{r},s), \tag{2}$$

where $w=w_A$ when $0<s<f_A$ and w_B when $f_A<s<1$. The initial condition of Eq. (2) satisfies $q(\mathbf{r},0)=1$. Because the two ends of the AB block copolymer are different, a second chain propagator $q^+(\mathbf{r},s)$ is needed which satisfies Eq. (2), with the right-hand side multiplied by -1 and the initial condition $q^+(\mathbf{r},1)=1$. The density of each component is obtained by

$$\phi_A(\mathbf{r}) = \frac{f_pV}{Q}\int_0^{f_A} dsq(\mathbf{r},s)q^+(\mathbf{r},s), \tag{3}$$

$$\phi_B(\mathbf{r}) = \frac{f_pV}{Q}\int_{f_A}^{1} dsq(\mathbf{r},s)q^+(\mathbf{r},s), \tag{4}$$

$$\phi_S(\mathbf{r}) = \frac{f_SV}{Q_S}\exp(-w_S(\mathbf{r})/N). \tag{5}$$

Minimization of the free energy with respect to density and pressure, $\delta F/\delta\phi=\delta F/\delta\xi=0$, leads to another four equations.

$$w_A(\mathbf{r}) = \chi_{AB}N\phi_B(\mathbf{r}) + \chi_{AS}N\phi_S(\mathbf{r}) + \xi(\mathbf{r}), \tag{6}$$

$$w_B(\mathbf{r}) = \chi_{AB}N\phi_A(\mathbf{r}) + \chi_{BS}N\phi_S(\mathbf{r}) + \xi(\mathbf{r}), \tag{7}$$

$$w_S(\mathbf{r}) = \chi_{AS}N\phi_A(\mathbf{r}) + \chi_{BS}N\phi_B(\mathbf{r}) + \xi(\mathbf{r}), \tag{8}$$

$$\phi_A(\mathbf{r}) + \phi_B(\mathbf{r}) + \phi_S(\mathbf{r}) = 1. \tag{9}$$

We solve Eqs. (3)–(9) directly in real space by using a combinatorial screening algorithm proposed by Drolet and Fredrickson.[23] The algorithm consists of randomly generating the initial values of the fields $w_i(\mathbf{r})$. Using a Crank–Nicholson scheme and an alternating-direct implicit (ADI) method,[24] the diffusion equations are then integrated to obtain q and q^+, for $0<s<1$. Finally, the right-hand sides of Eqs. (3)–(5) are evaluated to obtain new values for the volume fractions of blocks A, B, and solvent S. Moreover, the brief introduction of SCFT method can be found in some textbook, such as "Statistical Physics of Polymers: An Introduction."[25]

The numerical calculations were performed in two-dimensional space with $L\times W$ grid points in the xz plane. The surfaces were represented as lines with a thickness of 1 grid point and positioned at 0 and $W+1$. The interactions between the walls and the polymers are assumed to zero and only the confinement is considered here. The grid size $\Delta x=\Delta z=\Delta=0.5a$. Periodic boundary is used along the x direction, and the regions of $z<1$ and $z>W$ are forbidden, i.e., $q,q^+=0$ for $z<1$ and $z>W$. All calculations have been done

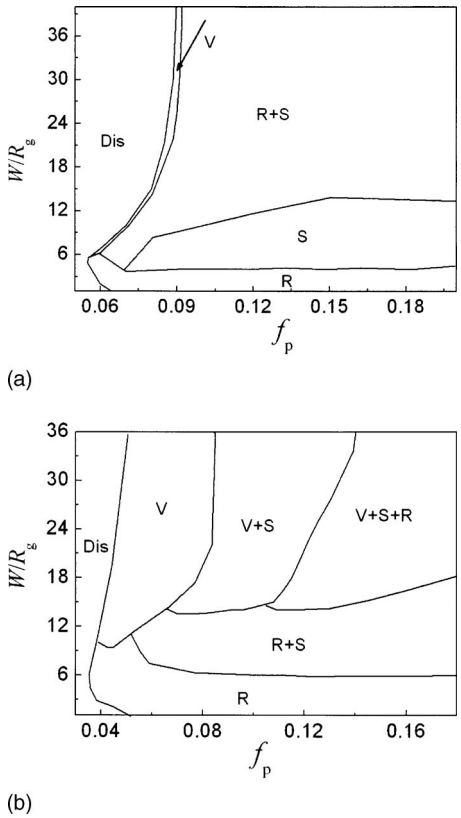

FIG. 1. Phase diagrams of confined asymmetric diblock copolymer in selective solvents as a function of W and f_p. The parameters are (a) $f_A=0.15$, $\chi_{AB}N=35$, $\chi_{AS}N=0.5$, $\chi_{BS}N=24$ and (b) $f_A=0.15$, $\chi_{AB}N=15$, $\chi_{AS}N=0.5$, $\chi_{BS}N=25$ (Ref. 21).

with $L=200$, which is much larger than the polymer radius of gyration (R_g) to avoid periodic boundary effects on the microstructure. Our simulation is performed using an initial random distribution of concentration with a fluctuation amplitude of $\Delta f_P=10^{-4}$ to ensure that the observed morphologies are independent of the initial condition, i.e., we control the initial density fluctuation within $\Delta f_P=10^{-4}$ because the initial fluctuation will affect the final structures.[12] The simulation is carried out until the phase patterns are stable and the free energy difference between two iterations is smaller than 10^{-6}, i.e., $\Delta F<10^{-6}$. All the simulations are repeated by using different random numbers to guarantee the observed structure are not artifacts.

Our calculations investigate the A_3B_{17} diblock copolymers ($f_A=0.15$) with a radius of gyration (R_g) of $1.826a$ in selective solvent. The interaction parameters are set to be the following: $\chi_{AB}N=35$, $\chi_{AS}N=0.5$, and $\chi_{BS}N=24$. Therefore, the solvent is good for block A, i.e., block A is hydrophilic and short enough to ensure the crew-cut aggregates are formed. The interaction between block A and B is stronger than our previous work, resulting in different phases.

III. RESULTS AND DISCUSSION

The phase diagram at $f_A=0.15$ with $\chi_{AB}N=35$, $\chi_{AS}N=0.5$, and $\chi_{BS}N=24$ is shown as a function of the concentration of block copolymer f_P and the film thickness W in Fig. 1(a). The lines represent the calculated theoretical phase boundaries. In this case, there are about five phase regions

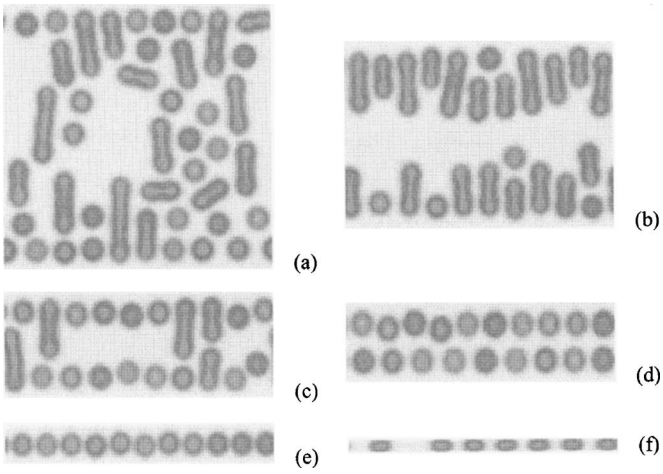

FIG. 2. Morphologies of the asymmetric AB diblock copolymers in selective solvent with different film thicknesses at $f_p=0.15$. (a) $W=200\Delta$ $(54.8R_g)$ (b) $W=140\Delta$ $(38.3R_g)$, (c) $W=80\Delta$ $(21.9R_g)$, (d) $W=60\Delta$ $(16.4R_g)$, (e) $W=30\Delta$ $(8.2R_g)$, and (f) $W=10\Delta$ $(2.7R_g)$. The black and gray colors represent the blocks A and B, respectively.

found in our simulation: Dis, V, R+S, S, and R, which correspond to the disordered phase, vesicles, mixtures of rods and spheres, spheres, and rods in three dimensional (3D), respectively. Compared to the phase diagram at $\chi_{AB}N=15$, $\chi_{AS}N=0.5$, and $\chi_{BS}N=25$ [see Fig. 1(b)],[21] the strong repulsion between A and B blocks has led to better miscibility with the solvent, as seen in the increase of the Dis region. The vesicle phase region is reduced, and the phases related to vesicles, such as (V+R+S, V+S) disappear. A new sphere phase (S), which maximizes the block A–solvent contact and minimizes the block B–solvent contact, is found.

The stable morphologies formed by the A_3B_{17} diblock copolymers in selective solvents for different film thicknesses at $f_P=0.15$ are shown in Fig. 2. In bulk solution, the block copolymers form a stable mixture of rodlike and spherelike micelles (R+S). The stable morphologies change with confinement. When the hard walls are far from each other, the morphology is similar to the one in bulk, see Fig. 2(a). As the film thickness decreases to $W=140\Delta(38.3R_g)$, the rods and the spheres are near the surface and the long axis of most rods tends to normal to the surfaces, as shown in Figs. 2(b) and 2(c). The free energy of the system will minimize when the rods are vertical to the surface because it decreases the polymer conformational frustration near the walls. The number of the rods decreases and the more spherelike micelles occur as film thickness W changes from 140Δ, to 80Δ, to 60Δ. The rods disappear when $W=60\Delta(16.4R_g)$, and two layers of spherelike micelles (S) are found. The layers of spherelike micelles decrease when W further decreases, and only the rodlike micelles are found if the confinement is less than four to five times R_g of the diblock copolymer [see Fig. 2(f)]. The rodlike micelles align parallel to the surface to avoid polymer conformational frustration.

Figure 3 shows the transition between different morphologies of the A_3B_{17} block copolymer in solution at $f_p=0.11$. The phase transition process is similar with the case for $f_p=0.15$. The only difference is that the patterns stay near the surfaces when the film thickness is large, such as

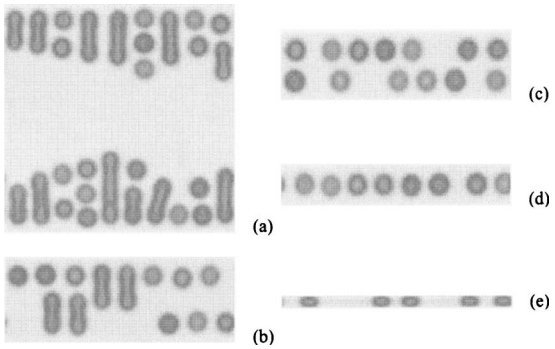

FIG. 3. Morphologies of the asymmetric AB diblock copolymers in selective solvent with different film thicknesses at f_p=0.11. (a) W=200Δ (54.7R_g), (b) W=75Δ (29.8R_g), (c) W=60Δ (16.4R_g), (d) W=35Δ (9.6R_g), and (e) W=10Δ (2.7R_g). The black and gray colors represent the blocks A and B, respectively.

W=200Δ(54.7R_g). It is because that the polymer chains at f_p=0.15 are more than those at f_p=0.11, and there is not enough space for the polymer stay near the surfaces. Figure 4 shows the morphology transitions of the A_3B_{17} block copolymer in solution at f_p=0.09. The disordered phase (Dis) is stable in the bulk. The disordered phase becomes unstable and the mixture of rodlike and spherelike micelles form when the film thickness decreases to W=176Δ(48.2R_g) although it is not a real thin film. When the boundary conditions are used, the disordered phase occurs at W=176Δ. The spherelike micelles (S) will form when W=60Δ (not shown in the figure), and the rodlike micelles (R) along the surfaces when the film thickness is four or five time of R_g, as shown in Fig. 4(d).

When we further decrease the concentration of block copolymers, f_p=0.07, the disordered phase is stable in the bulk. The phase transition occurs when the film thickness decreases to W=43Δ (11.8R_g). The spherelike vesicles form at the largest separation. The mixtures of the rodlike and spherelike micelles are stable when the film thickness decrease a little to W=42Δ (11.5R_g). The rodlike micelles along the surfaces form when the film thickness is four or five time of R_g, see Fig. 5(c).

For the systems here, the self assembled morphologies induced by the confinement stay near the surfaces within a distance of the radius of the gyration of polymers and the rod-like micelles tend to align normal to the surfaces when the film thickness is large enough ($W \gg 20R_g$). Here, we present the density profile along the z-direction to elucidate the surface phase separation. Figure 6 shows the density profile of the diblock copolymer along the z-direction at f_p=0.09 with W=200(54.8R_g) (solid), W=190(52.0R_g) (dash), and W=180Δ (49.3R_g) (dot). A depleted region of block copolymers of approximately R_g can be clearly seen near the surfaces. Polymer segments are excluded from the surface due to the conformational restrictions, leading to higher concentration of block copolymers far from the surfaces of the film. Interestingly, it can be seen that the polymer density exhibits a maximum at a distance of approximately 4–5R_g from the wall. Density oscillations in the polymer density profile near a wall has previously been observed in several other theoretical studies in polymer adsorption.[19,26] However, the magnitude of the density oscillation peak found in polymer adsorption are on the order of 0.1% at a distance less than R_g from the wall, which is related to the change of the polymer conformation near the walls, in contrast to the 5% peak observed here. The amplitude of the oscillations decays quickly with increasing distance z from the surface. The decay length, measure for the range of the ordering in polymer solution caused by the surface,[27] has the order of R_g, implying that the bump arises from correlations between polymer coils. By analogy with hard sphere fluids, the oscillatory behavior in segment density is associated with the liquid-like layering of polymer coils near the surface.[27] Increasing the confinement (decreasing the film thickness W) will amplify the oscillation and the position of the maximum amplitude shifts away from the planar wall. Therefore, the block copolymers self-assemble when the concentration of polymers at the maximum is larger than the critical micelle concentration (CMC ~ 0.103 in the bulk solution in this case).

Figure 7 presents the reduced density profiles of blocks

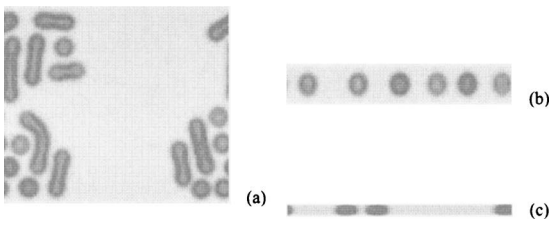

FIG. 4. Morphologies of the asymmetric AB diblock copolymers in selective solvent with different film thicknesses at f_p=0.09. (a) W=176Δ (48.2R_g), (b) W=36Δ (9.9R_g), and (c) W=10Δ (2.7R_g). The black and gray colors represent the blocks A and B, respectively.

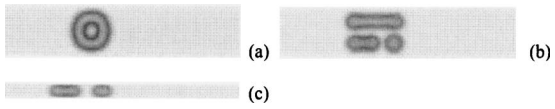

FIG. 5. Morphologies of the asymmetric AB diblock copolymers in selective solvent with different film thicknesses at f_p=0.07. (a) W=43Δ (11.8R_g), (b) W=42Δ (11.5R_g), and (c) W=12Δ (3.3R_g). The black and gray colors represent the blocks A and B, respectively.

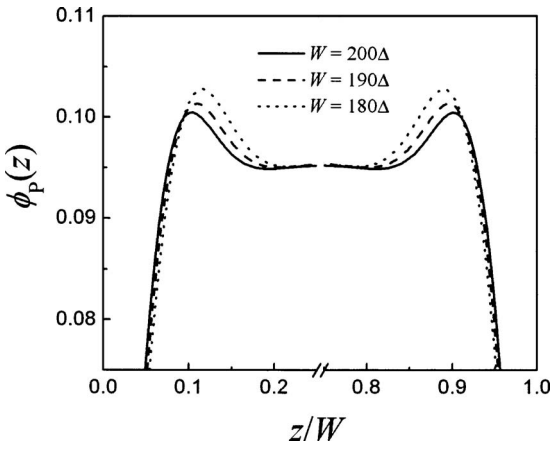

FIG. 6. Density profile of diblock copolymers perpendicular to the surfaces at f_p=0.09 with W=200Δ (54.8R_g) (solid), W=190Δ (52.0R_g) (dash), and W=180Δ (49.3R_g) (dot). The abscissa of the figure is reduced by W.

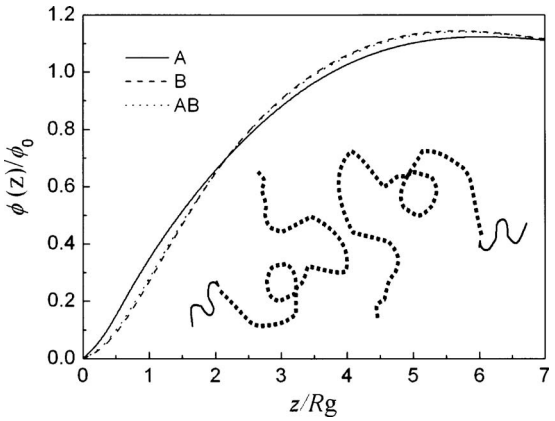

FIG. 7. Reduced density profiles of blocks A (solid), B (dash), and diblock copolymers (dot) perpendicular to the surfaces at $f_p=0.09$ with $W=180\Delta$ $(49.3R_g)$. The solid and dash lines in the inserted cartoon represent the blocks A and B, respectively.

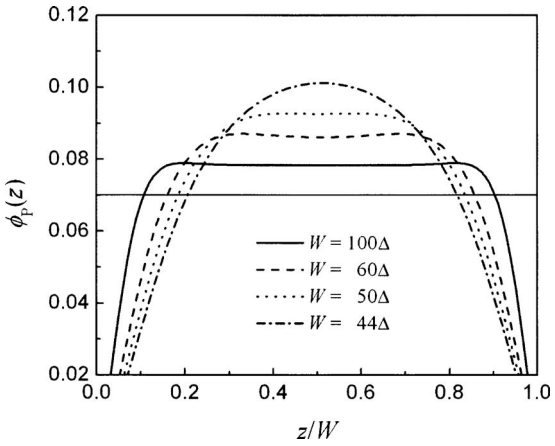

FIG. 8. Density profile of diblock copolymers perpendicular to the surfaces at $f_p=0.07$ with $W=100\Delta$ $(27.4R_g)$ (solid), $W=60\Delta$ $(16.4R_g)$ (dash), $W=50\Delta$ $(13.7R_g)$ (dot), and $W=44\Delta$ $(12.0R_g)$ (dash dot). The abscissa of the figure is reduced by W.

A(solid), B(dash), and diblock copolymers(dot) perpendicular to the surfaces at $f_p=0.09$ with $W=180\Delta(49.3R_g)$. The block A (hydrophilic) have higher density than block B (hydrophobic) closer to the surfaces due to less conformation restriction on the shorter block A near the walls. Although the interaction parameters between the blocks A and B, and the solvent is similar to our previous work ($\chi_{AS}N=0.5$, $\chi_{BS}N=25$),[21] the strong repulsion between the blocks A and B strengthens the repulsion between the hydrophobic block B and the solvent S due to a long, strongly hydrophobic segment B. There are two aspects for the large oscillation: (1) Compared with the block A, block B is more strongly depleted from the surface because of its longer length. (2) Due to its strong repulsion with block A, the neighboring block copolymer is more likely to have its B block facing the block copolymer closer to the wall, leading to a maximum of the block B density at approximately $5R_g$, which can be clearly shown by the inserted cartoon in Fig. 7. The strong repulsion between the solvent and the polymer leads to the large oscillation amplitude.[2,19] Therefore, the large density fluctuation near the surface occurs in this case mainly due to the strong repulsion between the blocks A and B.

But when the concentration of the diblock copolymers decreases, such as $f_p=0.07$, the oscillating behavior is not more obvious than that at $f_p=0.09$, as shown in Fig. 8. The transition from the disordered to the separated phase occurs only at the strong confinement (thinner film thickness), where the film thickness is below two times of the depletion layer thickness. The oscillation in polymer density is suppressed. From Fig. 5, we also can see that the self assembled morphology is at the center and not near the surface with a distance of R_g from the wall. Figure 8 shows that as the confinement effect increases from $W=100\Delta$ to 44Δ, the depletion region grows relative to the slit height (but remains approximately R_g), resulting in higher concentration of block copolymers in the center of the film and higher solvent concentration near the surfaces. Therefore, the block copolymers self-assemble when the concentration of polymers at the center of the slit is larger than the critical micelle concentration (CMC$\approx$0.103 in the bulk solution).

Even for the higher concentration condition, such as $f_p=0.15$ and $f_p=0.11$, the depletion-induced surface separation is also obvious. Figure 9 presents the density profiles of the block copolymer as a function of z for $f_p=0.15$, $L_z=140$ and $f_p=0.11$, $L_z=200$. For these polymer concentrations, the block copolymers can phase separate in the bulk. From Fig. 9, we can clearly see the large oscillations near the surface (with a distance of $4-5R_g$), which are consistent with Figs. 2(b) and 3(a). Due to the strong depletion effect, the density oscillation of the block copolymer near the surface is very high, which results in the higher density near the surface with a distance of $4-5R_g$.

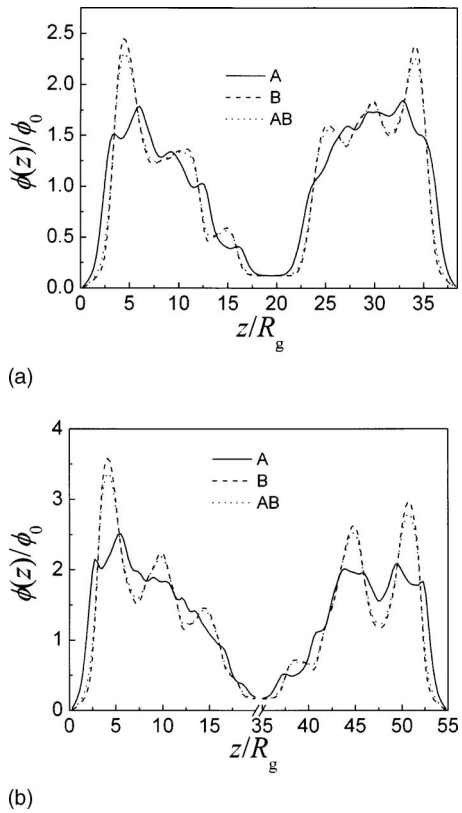

FIG. 9. Density profiles of diblock copolymers perpendicular to the surfaces for (a) $f_p=0.15$, $L_z=140$ and (b) $f_p=0.11$, $L_z=200$. The abscissa of the figure is reduced by R_g.

When the repulsive interaction between the blocks is strong, the vesicle is not as easily observed as in the weak segregation regime.[21] Due to the strong repulsion between the blocks A and B, the block copolymer phase separate easier than the separation between the block copolymers and the solvent. The mixture of vesicles, rodlike and spherelike micelles (V+R+S) and the mixture of vesicles and spherelike micelles are not observed in the strong segregation regime. Phase separation occurs near the surfaces due to the large oscillation of the block copolymer distribution along the z direction.

It is well known that the entropic polymer depletion affects the system phase behavior more strongly in dilute and semidilute solutions rather than in concentrated solutions.[19] In the following part, we provide insight by calculating the entropic contributions from the block copolymer and the solvent, as well as the enthalpy of the interfacial polymer-solvent and different block interactions, to elucidate how confinement affects the phase transition of the block copolymer. The entropy of a single block copolymer chain S/k_B is given by

$$\frac{S}{k_B} = \ln\left(\frac{Q_B}{f_P V}\right) + \frac{1}{f_P V}\int d\mathbf{r}(w_A\phi_A + w_B\phi_B). \tag{10}$$

Also, the entropy of a single solvent molecule S_S/k_B is

$$\frac{S_S}{k_B} = \ln\left(\frac{Q_S}{f_S V}\right) + \frac{1}{Nf_S V}\int d\mathbf{r}w_S\phi_S. \tag{11}$$

The interfacial energy F_{int} is described by

$$\frac{NF_{\text{int}}}{k_B T\rho_0 V} = \frac{1}{V}\int d\mathbf{r}(\chi_{AB}N\phi_A\phi_B + \chi_{AS}N\phi_A\phi_S + \chi_{BS}N\phi_B\phi_S) - F_{\text{int}}^0, \tag{12}$$

where F_{int}^0 is the reference interaction energy, which takes the form $F_{\text{int}}^0 = \chi_{AB}Nf_P^2 f_A f_B + \chi_{AS}Nf_P f_A f_S + \chi_{BS}Nf_P f_B f_S$.

Figure 10(a) shows the order-disorder transition of the block copolymer for $f_P=0.09$ at $W=176\Delta$ ($\sim 48.2R_g$), and $f_P=0.07$ at $W=43\Delta$ ($\sim 11.8R_g$) and corresponding sharps decrease in S/k_B. In this case, the decrease in polymer entropy is due to self-assembly of the block copolymer, which is induced by the polymer depletion effect. As shown in Figs. 6 and 8, the polymer concentration with a distance about R_g from the surfaces is greater than the critical micelle concentration, leading to the self-assembly of vesicle aggregates. As the confinement decreases further, the entropy of a single block copolymer chain S/k_B decreases with decreasing W, and very rapidly decrease at a film thickness of approximately $2-3R_g$. In such highly confined systems, the rodlike micelle morphology is stable due to the polymer conformational entropy loss. The entropy of a single solvent molecule S_S/k_B, in contrast to the polymer entropy, stays almost constant for varying slit height through different block copolymer morphologies, as shown in Fig. 10(b). S_S/k_B changes weakly only when $W \leqslant 5R_g$, and the depletion of polymers from the walls lead to higher local concentration of solvent molecules near walls. The interfacial energy change shown in Fig. 10(c) has the similar trend as the entropic free energy of the block copolymers, i.e., the rapid decrease occurs for $W<2-3R_g$. Comparing the magnitude of the polymer entropy change, the solvent entropy change, and the interfacial free energy change as the film thickness decreases, the change in the conformation entropy of the block copolymer besides the interfacial free energy is the dominant contribution that favors the rod micelle morphology for highly confined systems.

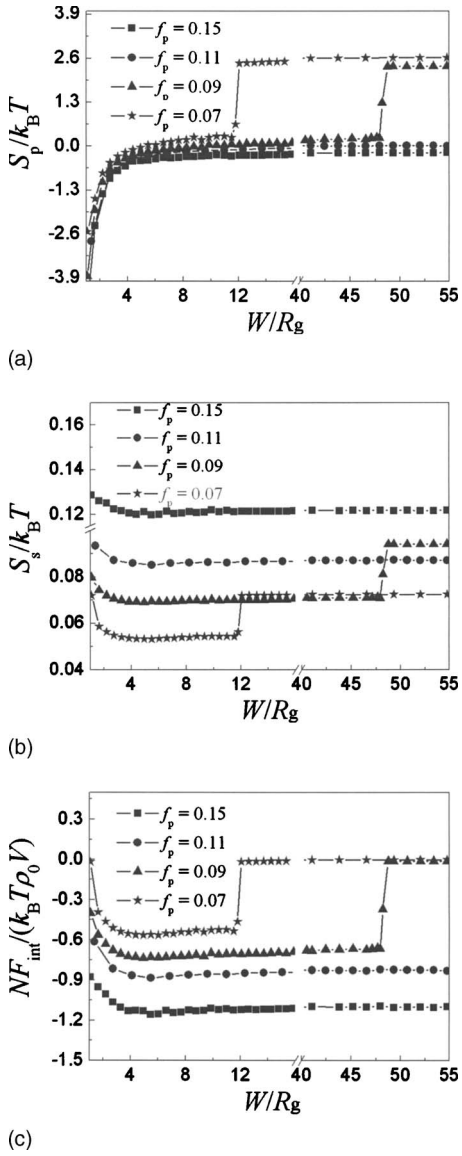

FIG. 10. (a) Entropy of a single block copolymer chain S/k_B, (b) entropy of a single solvent molecule S_S/k_B, and (c) interfacial energy $NF_{\text{int}}/(k_BT\rho_0V)$ as a function of the film thickness W for $f_p=0.15$ (squares), 0.11 (spheres), 0.09 (triangles), and 0.07 (stars).

In order to further elucidate the depletion-induced surface separation, we present the free energy as a function of z for $f_P=0.15$, $L_z=140$ and $f_P=0.41$, $L_z=200$ in Fig. 11. The results show that the free energy has the same phenomena with the density distribution which is shown in Fig. 9. The energy has the local minimum near the surface with a distance of $4-5R_g$.

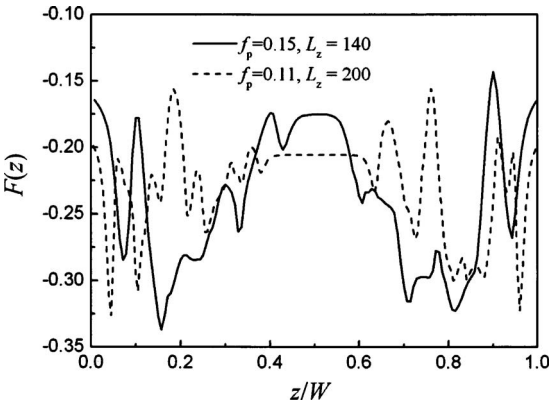

FIG. 11. Free energy of the system as a function of the z for f_p=0.15, L_z=140 (solid) and f_p=0.11, L_z=200 (dash).

IV. SUMMARY AND CONCLUSION

Depletion-induced surface phase transition of asymmetric diblock copolymer in selective solvents is investigated by using the real space version of self-consistent field theory (SCFT) following our previous work. Five phases are predicted by varying the film thickness and the concentration of block copolymers. The influences of the film thickness and the concentration of block copolymers on chain conformations, and interfacial free energy are studied systematically. The predictions show that increasing the confinement effect/reducing the film thickness has a strong influence on the morphologies of the block copolymer in selective solvents. In particular, the block copolymer is found to layer near the surface due to a long, strongly hydrophobic segment. This leads to polymer "packing" and density oscillations near the surface, allowing phase separation to occur when the local density is higher than the CMC.

At the highest polymer concentration f_P=0.15 and 0.11, as the slit height decreases, the morphologies change from S+R to S and finally to R. At f_P=0.09, the morphology varies from disordered to V to R+S to S and finally to R. At f_P=0.09, vesicle self assembly can be induced by confinement as the slit height decreases to W=176Δ, and it easily changes to mixture of rod-like and sphere-like micelles (R+S) when the film thickness decreases a little to W=170Δ. The morphology varies from R+S to S at W=60Δ and last to R. At f_P=0.07, the separated phase change from DIS to V to R+S and finally to R. These studies show that the block copolymer concentration also strongly affect the confinement-induced phase transition of block copolymers in solutions. Compared with the weak interaction between the different components of the block copolymer, the phase regions with vesicles are reduced and some phase (such as V+R+S, V+S) that can be seen in the weak segregation disappears.

A very interesting observation is that even for confinement that is much larger than the chain radius of gyration (W=48.2R_g), confinement effect alone can induce a phase separation when the copolymer concentration is just below the critical micelle concentration. Polymer depletion can clearly be seen near the surfaces, leading to higher concentration of block copolymers at approximately 5R_g from the surfaces of the film that is above the CMC. The block copolymers self assemble at a distance R_g from the walls. The rodlike micelles tend to align normal to the surfaces because of more conformational freedom away from the walls. In a highly confined solution ($W\sim 2-3R_g$), the entropy of the block copolymer dominates the change in micelle morphology because polymer chain conformations are highly restricted. The change in polymer conformation leads to the reduction of the morphology space, such that strong surface confinement can speed up rearrangement of the microdomains.

ACKNOWLEDGMENTS

This work has been supported by National Natural Science Foundations of China (Nos. 20674035, 20504013, and 50533020), Nanjing University Talent Development Foundation (No. 0205004107) and Natural Science Foundation of Nanjing University (No. 0205005216).

[1] S. Asakura and F. Oosawa, J. Chem. Phys. **22**, 1255 (1954); J. Polym. Sci. **33**, 183 (1958); D. S. Zhou, N. Xu, L. Li, G. Ji, and G. Xue, J. Phys. Chem. B **107**, 2748 (2003); J. van der Gucht, N. A. M. Besseling, and G. J. Fleer, Macromolecules **35**, 2810 (2002); G. J. Fleer, A. M. Skvortsov, and R. Tuinier, Macromol. Theory Simul. **16**, 531 (2007).
[2] G. J. Fleer, A. M. Skvortsov, and R. Tuinier, Macromolecules **36**, 7857 (2003).
[3] M. W. Matsen, J. Chem. Phys. **106**, 7781 (1997); T. L. Morkved and H. M. Jaeger, Europhys. Lett. **40**, 643 (1997); T. Geisinger, M. Muller, and K. Binder, J. Chem. Phys. **111**, 5241 (1999); **111**, 5251 (1999); K. O. Rasmussen, J. Polym. Sci., Part B: Polym. Phys. **42**, 3695 (2004); A. Horvat, A. Knoll, G. Krausch, L. Tsarkova, K. S. Lyakhova, G. J. A. Sevink, A. V. Zvelindovsky, and R. Magerle, Macromolecules **40**, 6930 (2007); S. Ludwigs, G. Krausch, R. Magerle, A. V. Zvelindovsky, and G. J. A. Sevink, *ibid.* **38**, 1859 (2005); K. S. Lyakhova, A. Horvat, A. V. Zvelindovsky, and G. J. A. Sevink, Langmuir **22**, 5848 (2006); T. Xu, A. V. Zvelindovsky, G. J. A. Sevink, K. S. Lyakhova, H. Jinnai, and T. P. Russell, Macromolecules **38**, 10788 (2005).
[4] H. P. Huinink, J. C. M. Brokken-Zijp, M. A. van Dijk, and G. J. A. Sevink, J. Chem. Phys. **112**, 2452 (2000); H. P. Huinink, M. A. van Dijk, J. C. M. Brokken-Zijp, and G. J. A. Sevink, Macromolecules **34**, 5325 (2001).
[5] S. H. Kim, M. J. Misner, and T. P. Russell, Adv. Mater. (Weinheim, Ger.) **16**, 2119 (2004); S. H. Kim, M. J. Misner, T. Xu, M. Kimura, and T. P. Russell, *ibid.* **16**, 226 (2004); H. Elbs, C. Drummer, V. Abetz, and G. Krausch, Macromolecules **35**, 5570 (2002); K. Fukunaga, H. Elbs, R. Magerle, and G. Krausch, *ibid.* **33**, 947 (2000); G. Kim and M. Libera, *ibid.* **31**, 2569 (1998); Y. Z. Chen, Z. B. Wang, Y. M. Gong, H. Y. Huang, and T. B. He, J. Phys. Chem. B **110**, 1647 (2006).
[6] J. P. Spatz, A. Roescher, S. Sheiko, G. Krausch, and M. Moller, Adv. Mater. (Weinheim, Ger.) **7**, 731 (1995); Z. Li, W. Zhao, M. H. Rafailovich, J. Sokolov, K. Khougaz, B. Lennox, A. Eisenberg, and G. Krausch, J. Am. Chem. Soc. **118**, 10892 (1996); B. H. Sohn, S. I. Yoo, B. W. Seo, S. H. Yun, and S. M. Park, *ibid.* **123**, 12734 (2001); J. C. Meiners, H. Elbs, A. Ritzi, J. Mlynek, and G. Krausch, J. Appl. Phys. **80**, 2224 (1996).
[7] M. W. Matsen, Curr. Opin. Colloid Interface Sci. **3**, 40 (1998); K. Binder, in *Polymers in Confined Environments* (Springer, Berlin/Heidelberg, 1999), p. 1.
[8] Q. Wang, P. F. Nealey, and J. J. de Pablo, Macromolecules **36**, 1731 (2003).
[9] Y. Z. Yang, F. Qiu, H. D. Zhang, and Y. L. Yang, Polymer **47**, 2205 (2006).
[10] G. Yu and A. Eisenberg, Macromolecules **31**, 5546 (1998); F. T. Liu and A. Eisenberg, J. Am. Chem. Soc. **125**, 15059 (2003).
[11] L. B. Luo and A. Eisenberg, J. Am. Chem. Soc. **123**, 1012 (2001); K. Yu and A. Eisenberg, Macromolecules **31**, 3509 (1998); S. Burke, H. W. Shen, and A. Eisenberg, Macromol. Symp. **175**, 273 (2001).
[12] X. H. He, H. J. Liang, L. Huang, and C. Y. Pan, J. Phys. Chem. B **108**, 1931 (2004).

[13] J. T. Zhu, Y. Jiang, H. J. Liang, and W. Jiang, J. Phys. Chem. B **109**, 8619 (2005); X. Li, P. Tang, F. Qiu, H. D. Zhang, and Y. L. Yang, *ibid.* **110**, 2024 (2006).
[14] R. Wang, P. Tang, F. Qiu, and Y. L. Yang, J. Phys. Chem. B **109**, 17120 (2005).
[15] G. J. A. Sevink and A. V. Zvelindovsky, Macromolecules **38**, 7502 (2005).
[16] L. F. Zhang and A. Eisenberg, Macromolecules **29**, 8805 (1996).
[17] C. Allen, D. Maysinger, and A. Eisenberg, Colloids Surf., B **16**, 3 (1999); Z. S. Gao and A. Eisenberg, Macromolecules **26**, 7353 (1993); D. E. Discher and A. Eisenberg, Science **297**(5583), 967 (2002).
[18] R. Tuinier, J. Rieger, and C. G. de Kruif, Adv. Colloid Interface Sci. **103**, 1 (2003).
[19] J. L. Hu, R. Wang, and G. Xue, J. Phys. Chem. B **110**, 1872 (2006).
[20] Y. Jiang, T. Chen, F. W. Ye, H. J. Liang, and A. C. Shi, Macromolecules **38**, 6710 (2005).
[21] R. Wang, Z. B. Jiang, Y. L. Chen, and G. Xue, J. Phys. Chem. B **110**, 22726 (2006).
[22] E. Helfand, J. Chem. Phys. **62**, 999 (1975).
[23] F. Drolet and G. H. Fredrickson, Phys. Rev. Lett. **83**, 4317 (1999); Macromolecules **34**, 5317 (2001).
[24] W. H. Press, B. P. Flannery, S. A. Teukolsky, and W. T. Vettering, *Numerical Recipes* (Cambridge Univeristy Press, Cambridge, England, 1989).
[25] T. Kawakatsu, *Statistical Physics of Polymers: An Introduction* (Springer-Verlag, Berlin, 2004).
[26] J. M. H. M. Scheutjens and G. J. Fleer, J. Phys. Chem. **83**, 1619 (1979); R. Maassen, E. Eisenriegler, and A. Bringer, J. Chem. Phys. **115**, 5292 (2001); J. van der Gucht, N. A. M. Besseling, J. van Male, and M. A. C. Stuart, *ibid.* **113**, 2886 (2000); P. G. Bolhuis, A. A. Louis, J. P. Hansen, and E. J. Meijer, *ibid.* **114**, 4296 (2001).
[27] J. van der Gucht, N. A. M. Besseling, J. van Male, and M. A. C. Stuart, J. Chem. Phys. **113**, 2886 (2000).